Glycobiology vol. 12 no. 8 pp. 499–505, 2002

The *Giardia intestinalis* filamentous cyst wall contains a novel β(1-3)-*N*-acetyl-D-galactosamine polymer: a structural and conformational study

Gerrit J. Gerwig[2], J. Albert van Kuik[2], Bas R. Leeflang[2], Johannis P. Kamerling[2], Johannes F.G. Vliegenthart[1,2], Craig D. Karr[3], and Edward L. Jarroll[3]

[2]Bijvoet Center, Department of Bio-Organic Chemistry, Section of Glycoscience and Biocatalysis, Utrecht University, Padualaan 8, NL-3584 CH Utrecht, The Netherlands; and [3]Department of Biology, Northeastern University, Boston, MA 02115, USA

Received on March 5, 2002; revised on April 2, 2002; accepted on April 3, 2002

Assembly of a protective cyst wall by *Giardia* is essential for the survival of the parasite outside the host intestine and for transmission among susceptible hosts. The structure of the *G. intestinalis* filamentous cyst wall was studied by chemical methods, mass spectrometry, and ^{1}H nuclear magnetic resonance spectroscopy. Isolated cyst wall material contains carbohydrate and protein in a ratio of 3:2 (w/w), and the carbohydrate moiety is composed of a β(1-3)-*N*-acetyl-D-galactopyranosamine homopolymer. Conformational analysis by molecular dynamics and persistence length calculations of GalNAc oligomers in solution demonstrated a flexible structure consisting of left- and right-handed helical elements. It is most likely that in the solid state, the polysaccharide forms ordered helices or possibly multiple helical structures having strong interchain interactions. The highly insoluble nature of the *Giardia* cyst wall must be due to these strong interchain interactions and, probably, a strong association between the carbohydrate and the protein moiety.

Key words: cyst wall/*Giardia* /^{1}H NMR spectroscopy/mass spectrometry/polysaccharide

Introduction

The parasitic protozoan *Giardia intestinalis* (syn. *G. duodenalis*, *G. lamblia*) is a widespread human pathogen, being a major cause of enteric disease in the world (Craun, 1990). Human giardiasis ranges from an asymptomatic, self-limiting disease to a chronic infection (Wolfe, 1990). Signs and symptoms include flatulence, diarrhea (often with steatorrhea), epigastric pain and distress, nausea, and weight loss (Ferguson *et al.*, 1990). Transmission of giardiasis often occurs by fecal–oral routes via infected water. The life cycle of *Giardia* consists of two morphologically distinct forms: (1) the trophozoite that is responsible for pathogenesis within the gastrointestinal tract, and (2) a dormant cyst that serves in the transmission of the parasite to new hosts (Adam, 1991). *Giardia* cysts, produced in response to bile, measure approximately 8×12 μm and contain a pair of trophozoites. The cyst wall is composed of an inner (double) membranous and an outer (0.3 μm thick) filamentous portion (Erlandsen *et al.*, 1996). The filaments measure 7–20 nm in diameter and are arranged in a tightly packed meshwork (Erlandsen *et al.*, 1989). The highly insoluble cyst wall is essential for survival of the parasite outside the host. Cysts display greater resistance than do trophozoites to chemical agents used for water disinfection and to chemotherapeutic agents routinely used in the treatment of giardiasis (Paget *et al.*, 1998). Consequently, encystment represents a potentially important site of chemotherapeutic attack.

For the study of the cytodifferentiation from trophozoite to cyst as well as for our study of the biogenesis of the *Giardia* cyst wall, detailed information of the molecular structure of the cyst wall material is a prerequisite. It is widely accepted that many protozoan cyst walls contain chitin, but there is little sound biochemical evidence supporting this assumption. Indeed, a series of histochemical and biochemical studies suggested that the cyst wall of *Giardia* was composed of chitin (reviewed in Jarroll and Paget, 1995). However, in a series of studies (Jarroll *et al.*, 1989; Manning *et al.*, 1992; Macechko *et al.*, 1992) focused on *G. intestinalis* and *G. muris*, it was demonstrated that the filamentous cyst walls contain carbohydrate and protein and that the major monosaccharide constituent is *N*-acetyl-galactosamine (GalNAc). Subsequently, these investigators have shown that GalNAc is synthesized *de novo* from endogenous glucose (Macechko *et al.*, 1992) via a pathway of inducible enzymes, which are transcriptionally as well as allosterically regulated (Van Keulen *et al.*, 1998; Bulik *et al.*, 2000), and that GalNAc is fixed into an insoluble polysaccharide by the action of "cyst wall synthase" (Jarroll and Paget, 1995). Considering the insolubility of the cyst wall and the abundance of GalNAc, it was suggested that the filaments are composed of a carbohydrate(polysaccharide)–protein complex. With respect to the carbohydrate component, this report presents results demonstrating conclusively that the *Giardia* cyst wall filaments are not composed of chitin but of a previously undescribed (β1-3)-linked GalNAc homopolymer. Furthermore, insight is provided into conformational aspects of this polysaccharide.

[1]To whom correspondence should be addressed; E-mail: j.f.g.vliegenthart@chem.uu.nl

Results

Analysis of filamentous cyst wall material

Giardia intestinalis cysts were homogenized, and cyst pellets were collected by centrifugation, then treated with sodium dodecyl sulfate (SDS), amyloglucosidase, papain, DNase, RNase, and proteinase K resulting in an unsoluble fine-powdered white material, denoted cyst wall material CWM).

Gas-liquid chromatography (GLC) analysis after methanolysis of CWM and subsequent derivatization (re-*N*-acetylation, then trimethylsilylation) revealed D-GalNAc to be the only monosaccharide constituent. The total carbohydrate content amounted 63% (w/w). GLC analysis after acid hydrolysis of CWM and subsequent derivatization (trimethylsilylation) indicated the presence of galactosamine (GalN). Protein determination of CWM revealed a protein content of 36% (w/w). Taking into account the carbohydrate and protein content of CWM and the fact that CWM is hydrolyzable under the methanolysis/hydrolysis conditions used (Kamerling and Vliegenthart, 1989), a high percentage of GalN as native monosaccharide constituent in CWM can be ruled out. The identity of the *N*-acyl group as *N*-acetyl was demonstrated by ^{1}H nuclear magnetic resonance (NMR) spectroscopy and mass spectrometry (MS) (*vide infra*). Therefore it can be assumed that the carbohydrate part of CWM is a polysaccharide built up (nearly completely) from GalNAc residues.

To generate soluble material, the highly insoluble CWM was partially hydrolyzed (PH) by repeated short treatments with 0.5 M trifluroacetic acid (TFA). The mixture obtained (CWM PH) was fractionated by gel filtration chromatography (Figure 1) yielding five fractions, denoted CWM PH 1–5, which were rechromatographed to obtain better defined fractions. Fraction CWM PH 5 contained free GalNAc according to monosaccharide and ^{1}H NMR analysis. MALDI-TOF-MS analysis of fraction CWM PH 4 (Figure 2) only showed the presence of the pseudomolecular ion $[M+Na]^+$ of $HexNAc_2$ at *m/z* 446.9. After reduction (CWM PH 4R), monosaccharide analysis revealed the occurrence of GalNAc and GalNAc-ol in the molar ratio of 0.9:1.0, whereas methylation analysis demonstrated the presence of terminal GalNAc and 3-substituted GalNAc-ol.

The ^{1}H-NMR spectrum of CWM PH 4R, depicted in Figure 3A, was completely assigned using 2D total correlation spectroscopy (TOCSY) and rotating frame nuclear Overhauser effect spectroscopy (ROESY) measurements [GalNAc(β1-: H-1, δ 4.531, $J_{1,2}$ = 8.3 Hz; H-2, δ 3.898; H-3, δ 3.796; H-4, δ 3.913; H-5, δ 3.711; H-6a,6b, δ ~3.80; NAc, δ 2.084. -3)GalNAc-ol: H-1a,1b, δ ~3.60; H-2, δ 4.290; H-3, δ 3.999; H-4, δ 3.545; H-5, δ 4.198; H-6a,6b, δ ~3.65; NAc, δ 2.040. ROESY for GalNAc H-1, GalNAc-ol H-3]. Based on these results, fraction CWM PH 4R turned out to contain GalNAc(β1-3)GalNAc-ol.

In the MALDI-TOF-MS spectrum of fraction CWM PH 3 (Figure 2) mainly the pseudomolecular ion $[M+Na]^+$ of $HexNAc_3$ at *m/z* 650.0 is present; minor products are $HexNAc_2$ and $HexNAc_4$. Reduction (CWM PH 3R) followed by monosaccharide analysis showed the presence of GalNAc and GalNAc-ol in the molar ratio of 1.9:1.0, whereas methylation analysis showed the partially methylated alditol acetates of terminal GalNAc, 3-substituted GalNAc and 3-substituted

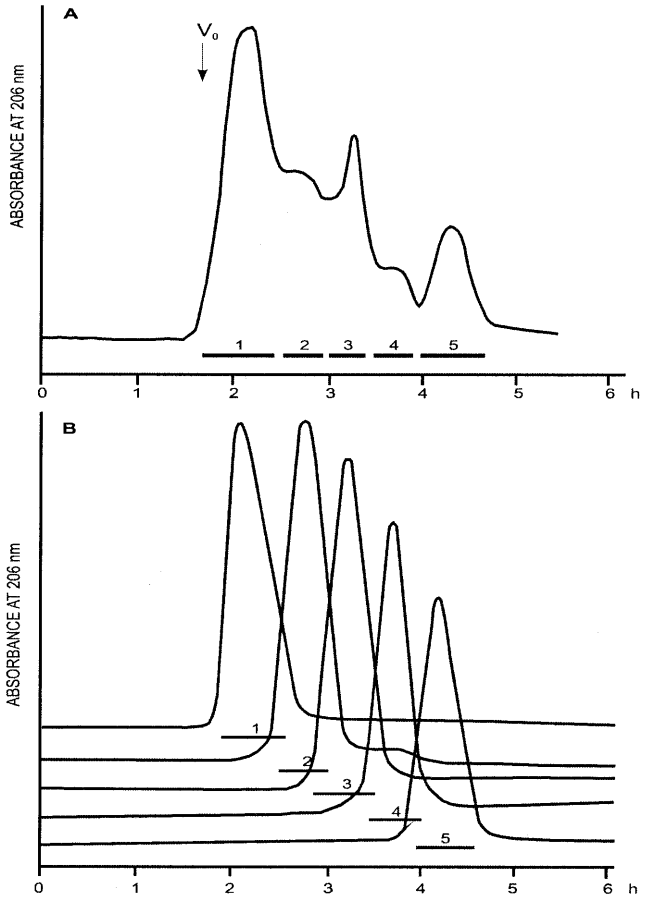

Fig. 1. Elution profile of partially hydrolyzed cyst wall material (CWM PH) on Bio-Gel P-2. (**A**) The column (68 × 1.6 cm) was eluted with H_2O at a flow rate of 22 ml/h. Fractions were collected as indicated. (**B**) Fractions were rechromatographed to obtain better defined fractions under the same conditions.

GalNAc-ol. Based on these results, fraction CWM PH 3R contains mainly GalNAc(β1-3)GalNAc(β1-3)GalNAc-ol. MALDI-TOF-MS analysis of fraction CWM PH 2 (Figure 2) showed the pseudomolecular ions $[M+Na]^+$ of oligosaccharides ranging from $HexNAc_4$ (*m/z* 852.8) up to $HexNAc_9$ (*m/z* 1868.0) (Δ *m/z* = 203). Methylation analysis of fraction CWM PH 2 showed besides terminal GalNAc, only 3-substituted GalNAc.

Monosaccharide analysis of fraction CWM PH 1 demonstrated a carbohydrate (GalNAc) content of 40% (w/w), whereas methylation analysis again showed only terminal GalNAc and 3-substituted GalNAc. The protein determination of CWM PH 1 showed a protein content of 60% (w/w). In the MALDI-TOF-MS spectrum of CWM PH 1 (Figure 2) a series of pseudomolecular ions $[M+Na]^+$ of oligosaccharides ranging from $HexNAc_5$ up to $HexNAc_{23}$ (*m/z* 4710.2) was observed. Because chain cleavage occurred during partial hydrolysis, the degree of polymerization in the native cyst wall material may be much higher.

The 1D ^{1}H-NMR spectrum of CWM PH 1 (carbohydrate region) is shown in Figure 3B, and the included proton assignments were obtained through analysis of 2D TOCSY and nuclear Overhauser effect spectroscopy (NOESY) NMR spectra. According to the various data, it can be concluded that the carbohydrate

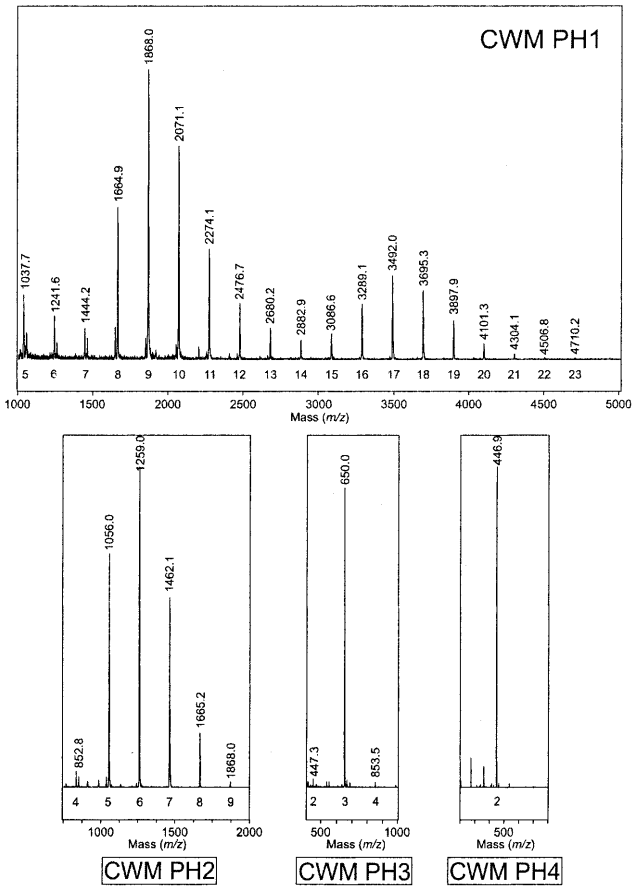

Fig. 2. MALDI-TOF mass spectra of CWM PH 1–4. The spectrum of CWM PH 1 contains the pseudomolecular ions $[M+Na]^+$ of GalNAc oligosaccharides ranging from 5 up to 23 residues. CWM PH 3 and PH 4 contain mainly a tri- and disaccharide, respectively.

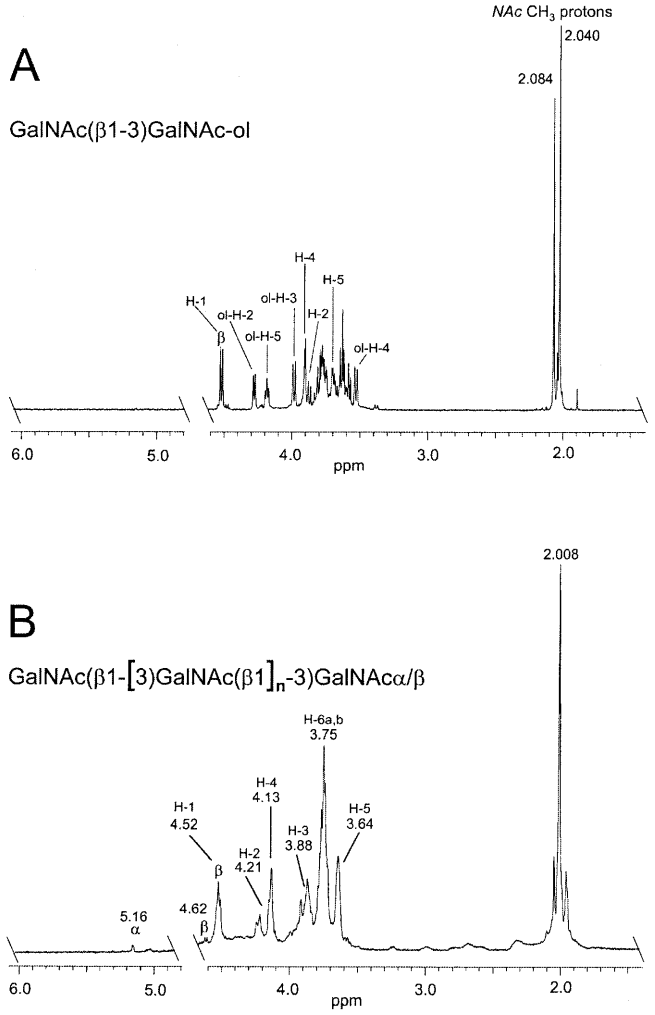

Fig. 3. 500-MHz ^{1}H NMR spectra of derived fractions from partially hydrolyzed CWM. (**A**) CWM PH 4R; (**B**) CWM PH 1. Spectra were recorded in D_2O at 300 K.

moiety of CWM is composed of a (β1-3)-linked GalNAc homopolymer. The structural analysis has been performed on GalNAc oligosaccharides released by partial acid hydrolysis, but in view of the high protein content in CWM PH 1, it is likely that a covalent linkage between protein and GalNAc oligomers occurs in CWM.

Conformational analysis of the carbohydrate moiety

To gain insight into the conformational aspects of the GalNAc polysaccharide, especially in relation to its insolubility, molecular dynamics (MD) calculations with the constituting disaccharide GalNAc(β1-3)GalNAc were performed. The results were used to evaluate possible conformations of polysaccharide structures.

To explore the preferred conformations of the glycosidic linkages φ (O5′-C1′-O3-C3) and ψ (C1′-O3-C3-C2) (IUPAC-IUB Joint Commission on Biochemical Nomenclature. , 1983), a relaxed energy map of the methyl glycoside of the disaccharide in vacuum was constructed with the use of the CHEAT force field (Grootenhuis and Haasnoot, 1993; Kouwijzer and Grootenhuis, 1995). This map (Figure 4A) showed two conformational regions with a low energy, one (φ, ψ = –60, –120) is

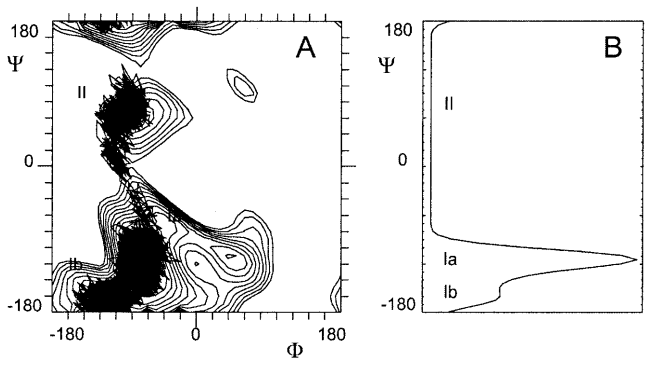

Fig. 4. Conformational analysis. (**A**) Result of a 3.5-ns GROMOS MD simulation of the GalNAc(β1-3)GalNAc disaccharide, started from region II. The trajectories for the interglycosidic linkages φ/ψ are projected on top of the energy contour map. The low-energy regions Ia, Ib, and II are indicated in the plot. (**B**) Probability distribution profile of the orientation of the ψ dihedral angle in the disaccharide, as calculated from the method of adaptive umbrella sampling of the potential of mean force.

denoted region I, and the other (φ, ψ = –60, 60) is denoted region II. Region I represents the global lowest energy. Next, minimal energy conformations selected from regions I and II were minimized again, this time with fully relaxed interglycosidic dihedral angles.

The conformational aspects of the disaccharide in solution were studied by two MD calculations in water, performed with the GROMOS force field (Spieser *et al.*, 1999). One run was started with the minimum energy conformation obtained from region I and was continued for 5 ns. The other simulation started with the lowest energy conformation from region II and had a duration of 3.5 ns. During this last simulation, the ψ dihedral angle changed after 500 ps simulation time from 60° (region II) to the global minimum at –120° (region I). The GalNAc(β1-3)GalNAc interglycosidic dihedral angles φ and ψ for this run are shown in Figure 4A, superimposed over the energy contour map. From this map it appears that the global energy minimum consists of two subminima, denoted region Ia and region Ib. The MD simulation that was started from region I did not visit region II. This run also showed the two regions Ia and Ib.

To assess the value of the computer simulation results, the ^{1}H NMR data of fraction CWM PH 1 were used. The NOESY spectra contained several medium to strong cross-peaks that in many cases were intraresidual. The H1′-H4 interaction would be detectable for the regions Ib (strong) and II (weak). Its absence however, demonstrated the dominant role of the Ia conformation. Signal overlap prevented a straightforward quantitative analysis of the NOEs.

To determine the population distribution of conformations more precisely, the method of adaptive umbrella sampling of the potential of mean force (Hooft *et al.*, 1992) was used. With this method, free energy differences are calculated between conformations in relation to the interglycosidic dihedral angle ψ. From this information, the population distribution of the conformations can be determined and this result is shown in Figure 4B. Inspection of this distribution profile shows that the GalNAc disaccharide only occurs in the global lowest energy conformation (region I). This energy minimum can be subdivided into two subminima, which are populated in a ratio of 4:1. Although the two conformations do not differ a great deal with respect to the interglycosidic dihedral angles, this small difference can have a significant effect on the total conformation of the GalNAc polysaccharide.

To get an impression of the conformation of this polysaccharide in solution, some polysaccharide models with a size of 30 monosaccharide units were constructed from disaccharides and linkage information obtained from the MD runs. Polysaccharide models constructed from disaccharide residues collected from region Ia form a right-handed helical structure. The average size of a helical turn is approximately seven residues. In contrast, polymer models constructed from disaccharide residues and linkages collected from region Ib gave a left-handed helical structure with an average helical-turn size of about 8.4 residues. A polysaccharide model chain, constructed from disaccharide structures and linkages selected from both regions in a ratio of Ia:Ib = 4:1, showed a random coil with a much more folded (less rodlike) conformation than observed for the two previous polysaccharide models (Figure 5).

To estimate the flexibility and to compare the stiffness of the three polysaccharide model structures mentioned, the persistence length (Kroon-Batenburg *et al.*, 1997) for all three polysaccharide

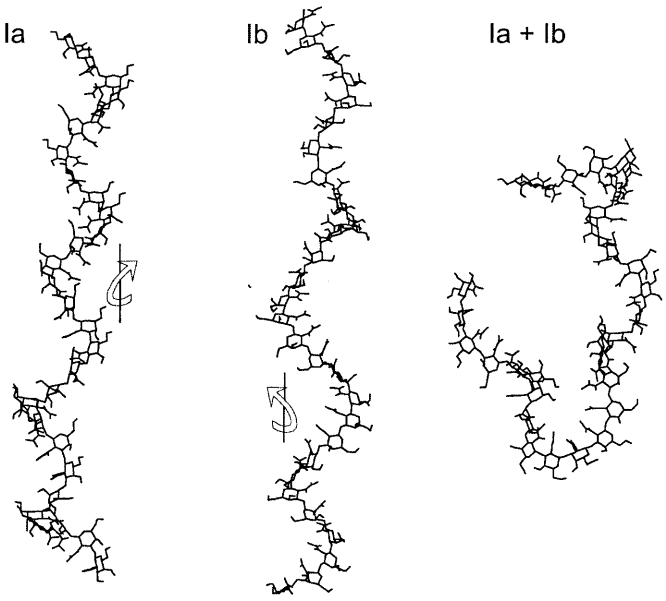

Fig. 5. Model polysaccharide chains constructed from disaccharides and linkage information randomly selected from appropriate conformational regions. All polysaccharides contain 30 monosaccharide residues. The polymer constructed from region Ia forms a right-handed (clockwise) helix, whereas the polymer built from region Ib has a left-handed helical conformation. The polysaccharide assembled from regions Ia and Ib (4:1) shows a random coil conformation.

model chains was calculated. The persistence length is the mean length of projection of a polymer chain along the direction of the first linkage and is a measure of the stiffness of the polymer. It is larger for stiffer chains. Polymers built exclusively from regions Ia or Ib have a persistence length of 52 and 80 Å, respectively. Calculations on a mixture of both regions in a ratio of Ia:Ib = 4:1, yielded a persistence length of 35 Å. Thus the combination of two different conformations results in a much more flexible chain. This flexibility is in agreement with the finding that polysaccharide fragments with a size of 23 monosaccharide units can still be dissolved in water. Compare, for example, cellulose, which has a persistence length in water in the order of 90–125 Å (Kroon-Batenburg *et al.*, 1997), and a largest dissolving fragment of nine monosaccharides. From these findings, it is evident that the highly insoluble character of the cyst wall cannot be accounted for by the conformational aspects of a single GalNAc polysaccharide chain but must be the result of strong interchain interactions. It is likely that the polysaccharide forms ordered helices in the solid state, possibly forming multiple helical structures, as is observed for similar polysaccharides, for example, (1-3)-linked β-D-GlcNAc (Kouwijzer and Perez, 1998; Rao *et al.*, 1998).

Discussion

The precursor for the GalNAc polymer is UDP-GalNAc, which is synthesized from endogenous glucose by inducible enzymes during encystment (Macechko *et al.*, 1992; Van Keulen *et al.*, 1998; Bulik *et al.*, 2000). Evidently, GalNAc is polymerized into a β(1-3)-D-Gal*p*NAc homopolymer by an

enzyme activity tentatively referred to as "cyst wall synthase" (Jarroll and Paget, 1995) and incorporated into an insoluble material resembling *Giardia*'s cyst wall filaments.

In our conformational studies, two preferential structures could be identified for GalNAc(β1-3)GalNAc. A 4:1 combination of these two conformations resulted in a flexible, random-coil model for the GalNAc polymer. From the conformational studies, it is clear that the highly insoluble nature of the cyst wall does not stem from the conformational properties of a single GalNAc polysaccharide chain but must be due to strong interchain interactions. The potential covalent linkage between the GalNAc polymers and the detected protein could also play a role. This is currently the subject of further study.

Of biological interest here is the fact that the cyst wall filaments of *Giardia* are not composed of chitin but rather of a novel polysaccharide for which no known degradative enzyme has been found as yet. Because many of the microorganisms that inhabit the intestines where these cysts are formed can produce chitinase, there could be a clear evolutionary advantage to *Giardia* not having its protective cyst wall composed of chitin. It is also interesting to speculate that since the cyst wall of *Giardia* is made of this novel GalNAc homopolymer, then there must be some hydrolase(s) capable of degrading it. Whether this hydrolase exists and is involved in the cytodifferentiation called excystation (trophozoites emerging from the cyst) is unknown. It is possible that excystation might occur simply by proteolysis of the protein present in the cyst wall as suggested by Ward *et al.* (1997). However, it is also likely that there exists a hydrolase capable of degrading this polymer, otherwise the amount of this material in the ecosystem would tend to accumulate irreversibly.

Materials and methods

Isolation and purification of Giardia cyst wall material

Approximately 40 L of *G. intestinalis* (strain MR4) trophozoites were grown in axenic culture and encysted for 24–48 h as described elsewhere (Macechko *et al.*, 1992). Cysts were collected by centrifugation of encystment medium at 750 × *g* for 10 min at 25°C and subjected to homogenization to disrupt trophozoites and partially encysted cells. Cyst pellets were washed five times in 10 ml distilled water and collected at 500 × *g*. Cyst wall filaments preparations were made by a modification of the procedure of Manning *et al.* (1992). The pooled sample was divided into two equal portions and processed separately. Each cyst pellet was heated to 100°C in an equal volume of 10% SDS for 5 min.

The cysts were concentrated by centrifugation at 12,000 × *g* for 5 min (as in subsequent steps), and the supernatant was discarded. The cyst pellet was washed in 10 ml distilled water five times until there were no visible signs of the detergent. The resulting cyst pellet was resuspended in 3 ml of amyloglucosidase buffer (20 mM acetate buffer, pH 4.5), transferred to a 20-ml glass screw-capped scintillation vial with a flat bottom and a stir bar. One hundred units of amyloglucosidase (EC 3.2.1.3, Sigma A-3514, St. Louis, MO) was added to the vial that was placed on a stir plate in a 55°C warm air incubator for 60 min. This procedure was repeated once more, and each time the supernatant was discarded.

After the two amyloglucosidase treatments, the SDS treatment was performed once again. The resulting cyst pellet was washed in 10 ml of freshly made papain buffer (100 mM phosphate buffered saline [PBS], pH 7.2, with 5 mM cysteine and 5 mM ethylenediamine tetra-acetic acid [EDTA]). The pellet was resuspended in 3 ml papain buffer and again placed in a glass scintillation vial with a stir bar. The sample was stirred with 50 U of papain (EC 3.4.22.2, Sigma P-4762) for 3 h at 60°C. This procedure was repeated once more, and each time the supernatant was discarded. Again the resulting cyst pellet was collected by centrifugation and washed, as in step one, with 10% SDS and water.

The pellet resulting from the papain treatment was subjected to DNase (EC 3.1.21.1, Sigma DN-25) and RNase (EC 3.1.27.5, Sigma R-4875) treatments. The pellet was resuspended in 3 ml of XNase buffer (0.1 M PBS, pH 7.2, with 5 mM $MgCl_2$) in a glass scintillation vial with a stir bar. The sample was incubated with 500 Kunitz units of DNase and 5 Kunitz units of RNase stirring for 2 h at 37°C. This treatment was repeated once more and the pellet washed with amyloglucosidase buffer. At this point, all subsequent centrifugation steps were carried out at 44,000 × *g* for 10 min at 10°C. Following the DNase/RNase treatment, the pellet was subjected to another amyloglucosidase treatment as described and then to a proteinase K (EC 3.4.21.14, Sigma P-0390) treatment. The pellet was washed once in proteinase K buffer (50 mM Tris, pH 8.0, 0.2% Triton X-100, 1 mM $CaCl_2$). The pellet was resuspended in the proteinase K buffer, placed in a glass scintillation vial with 50 U proteinase K, and stirred for 2 h at 60°C. This procedure was repeated once more, and the pellet was washed with an equal volume of 10% SDS containing 100 mM dithiothreitol (DTT) for 5 min at 100°C. The pellet was then washed five times in distilled water to remove the detergent and DTT. The resulting CWM was lyophilized for 48 h, yielding approximately 150 mg dry fine-powdered white material.

Monosaccharide analysis and protein determination

Monosaccharide analysis after methanolysis, re-*N*-acetylation, and trimethylsilylation, including absolute configuration determination using (-)-2-butyl glycosides, was performed by GLC-MS as described (Gerwig *et al.*, 1979; Kamerling and Vliegenthart, 1989). Protein determinations were carried out using a Micro BCA™ Protein Assay Reagent Kit (Pierce).

Acid hydrolysis

Dried CWM (1 mg) and GalNAc (1 mg) were each treated with 1 ml of 2 M HCl for 3 h at 100°C and with 1 ml of 4 M TFA for 5 h at 100°C. After lyophilization, the residues were dissolved in 1 ml H_2O. Aliquots of 25 µl of the four samples were taken, lyophilized, and trimethylsilylated with 25 µl pyridine/hexamethyldisilazane/chlorotrimethylsilane 5:1:1 (v/v) for 30 min at room temperature. Of each sample, 1 µl was analyzed by GLC (Chrompack CP 9002 gaschromatograph with CP Sil 5CB column, 25 m × 0.32 mm); temperature program: 140–240°C at 4°C/min).

Partial acid hydrolysis

Dried CWM (8 mg) was treated with 0.5 ml of 0.5 M TFA for 15 min at 100°C. After centrifugation, the supernatant was collected and the sediment was treated again with 0.5 ml of 0.5 M TFA for 15 min at 100°C. This procedure was repeated

several times until no sediment was left. Then, the total supernatant was concentrated by a stream of N_2 and lyophilized twice. The residue was suspended in 2 ml H_2O and filtered through a 0.22-µm Millex-GS filter (Millipore); the filtrate was fractionated on a column (68 × 1.6 cm) of Bio-Gel P-2 (Bio-Rad), using bidistilled H_2O as eluent (22 ml/h) and UV monitoring at 206 nm. Definite fractions (Figure 1) were rechromatographed on the same column.

Methylation analysis

Permethylation was performed essentially as described (Ciucanu and Kerek, 1984). Dried sample (0.1–1.0 mg) was dissolved in 1 ml dry dimethyl sulfoxide by ultrasonication for 30 min at 40°C. Freshly powdered NaOH (~10 mg) was added under an inert atmosphere, and the mixture was sonicated for 20 min at room temperature. After cooling to 0°C, 400 µl methyl iodide was added, and sonication was continued for 30 min at a temperature not exceeding 20°C. The latter step was repeated with a second addition of 400 µl methyl iodide. Then, 1 ml H_2O containing a few crystals of sodium thiosulfate was added, and the methylated product was isolated by extraction with chloroform (3 × 0.5 ml). The organic phase was washed with water (3 × 0.5 ml) and concentrated under a stream of N_2. The residue was hydrolyzed with 1 ml of 4 M TFA (4 h, 100°C) and, after coevaporation with methanol, reduced with $NaBD_4$ in water (2 h, room temperature). The excess of reductant was destroyed by the addition of 2 M acetic acid. Boric acid was removed by repeated evaporations with methanol. The sample was finally acetylated with 0.5 ml pyridine/acetic anhydride 1:1 (v/v) for 30 min at 100°C. The solvent was evaporated by a gentle stream of N_2 with intermediate addition of one drop of toluene, and the residue was redissolved in dichloromethane. The partially methylated alditol acetates were analyzed by GLC-MS (Kamerling and Vliegenthart, 1989).

MALDI-TOF MS

Positive-ion MALDI-TOF mass spectra were obtained on a Voyager-DE (PerSeptive Biosystems) instrument operating at an accelerating voltage of 21 kV (grid voltage 95%, ion guide wire voltage 0.05%) and equipped with a VSL-337ND-N_2 laser. The samples were dissolved in H_2O (1 µg/µl) and mixed with 2,5-dihydroxybenzoic acid (10 mg/ml) in a ratio of 1:2. Recorded data were processed using GRAMS/386 software (v. 3.04, Galactic Industries).

^{1}H NMR spectroscopy

Samples were exchanged twice in D_2O (99.9 atom% D, Isotec) with intermediate lyophilization. Finally, the material was dissolved in 0.5 ml of D_2O (99.96 atom% D, Isotec). One-dimensional resolution-enhanced 500-MHz ^{1}H-NMR spectra were recorded on a Bruker AMX-500 spectrometer at a probe temperature of 300 K. Chemical shifts are expressed in ppm by reference to internal acetone (δ 2.225) (Vliegenthart *et al.*, 1983). 2D TOCSY spectra with mixing times of 12, 25, 41, 50, and 125 ms were recorded at 500 MHz on a Bruker DRX-500 instrument. The spectra were processed using locally developed NMR software (Van Kuik, Bijvoet Center, Utrecht University). 2D ROESY experiments were carried out at 280 K with mixing times of 100, 200, 300, and 500 ms. The HOD signal was presaturated for 1 s during the relaxation delay.

Minimum energy calculations

Minimum energy calculations *in vacuo* were performed with CHEAT (Grootenhuis and Haasnoot, 1993; Kouwijzer and Grootenhuis, 1995), a CHARMm-based force field for carbohydrates in which hydroxyl groups are represented by extended atoms to prevent the formation of intramolecular hydrogen bonds and whereby energies are independent of the hydroxyl group orientation. A relaxed energy map was generated for the GalNAc(β1-3)GalNAc disaccharide by changing the inter-residual torsion angles in steps of 10° resulting in a 36 × 36 grid. For each grid point calculation, three intraglycosidic dihedral angles per monosaccharide ring and both interglycosidic angles are kept fixed by setting constraints during a first minimization. Next, all constraints in the ring were removed and the molecule was minimized a second time. Contour levels were plotted in steps of 1 kcal/mol from the global minimum.

Molecular dynamics calculations

Molecular dynamics simulations were carried out using the GROMOS program package (Van Gunsteren, 1987) and the updated carbohydrate force field for GROMOS (Spieser *et al.*, 1999) on local PentiumII class computers running Linux. Each molecule was surrounded by SPC/E (Berendsen *et al.*, 1987) water molecules and placed in a truncated octahedral periodic box. All bond lengths were kept fixed using the SHAKE procedure (Ryckaert *et al.*, 1977). A cut-off radius of 0.8 nm and a time step of 2 fs were used. Simulations were performed with loose coupling to a pressure bath at 1 atm and a temperature bath at 300 K (Berendsen *et al.*, 1984) with time constants of 0.5 and 0.1 ps, respectively. To confirm calculated data, (β1-3)-linked GalNAc oligosaccharide fragments with DP ~5 and DP >20 were analyzed by ^{1}H NMR spectroscopy.

Potential of mean force calculations on the GalNAc-GalNAc ψ glycosidic linkage

To calculate the free energy differences of the conformations around the GalNAc(β1-3)GalNAc glycosidic ψ angle, potential-of-mean-force calculations (Hooft *et al.*, 1992) were run for the methyl β-glycoside of the disaccharide with the GROMOS force field. All simulations were divided into jobs of 10 ps. The ψ values were collected into 72 classes, each with a width of $\Delta\psi = 5°$. The derivatives were fitted to a 12-term Fourier series. The first 0.2 ps of each job were discarded.

Persistence length calculations

The persistence length calculations of the GalNAc polymer were performed with data selected from appropriated parts of the MD simulations of the GalNAc(β1-3)GalNAc disaccharide (Kroon-Batenburg *et al.*, 1997). For each calculation, 1000 frames were selected and used to create chains of 300 residues.

Acknowledgments

We acknowledge partial support for this project from the NIH AI 41230 and the Netherlands Organisation for Scientific Research (NWO).

Abbreviations

CWM, cyst wall material; DTT, dithiothreitol; EDTA, ethylenediamine tetra-acetic acid; GalNAc, *N*-acetyl-D-galactosamine; GalN, D-galactosamine; GLC, gas-liquid chromatography; MALDI-TOF, matrix-assisted laser desorption ionization time-of-flight; MD, molecular dynamics; MS, mass spectrometry; NMR, nuclear magnetic resonance; NOESY, nuclear Overhauser effect spectroscopy; PBS, phosphate buffered saline; PH, partially hydrolyzed; ROESY, rotating frame nuclear Overhauser effect spectroscopy; SDS, sodium dodecyl sulfate; TFA, trifluoracetic acid; TOCSY, total correlation spectroscopy.

References

Adam, R.D. (1991) The biology of *Giardia* spp. *Microbiol. Rev.*, **55**, 706–732.

Berendsen, H.J.C., Postma, J.P.M., van Gunsteren, W.F., DiNola, A., and Haak, J.R. (1984) Molecular mechanics with coupling to an external bath. *J. Chem. Phys.*, **81**, 3684–3690.

Berendsen, H.J.C., Grigera, J.R., and Straatsma, T.P. (1987) The missing term in effective pair potentials. *J. Phys. Chem.*, **91**, 6269–6271.

Bulik, D.A., Van Ophem, P., Manning, J.M., Shen, Z., Newburg, D.S., and Jarroll, E.L. (2000) UDP-*N*-acetylglucosamine pyrophosphorylase, a key enzyme in encysting *Giardia*, is allosterically regulated. *J. Biol. Chem.*, **275**, 14722–14728.

Ciucanu, I. and Kerek, F. (1984) A simple and rapid method for the permethylation of carbohydrates. *Carbohydr. Res.*, **131**, 209–217.

Craun, G.F. (1990) Waterborne giardiasis. In: Meyer, E.A. (ed.), *Giardiasis*. Elsevier Science Publ. B.V., Amsterdam, pp. 267–293.

Erlandsen, S.L., Bemrick, W., and Pawley, J. (1989) High resolution electron microscopic evidence for the filamentous structure of the cyst wall in *Giardia muris* and *Giardia duodenalis*. *J. Parasitol.*, **75**, 787–797.

Erlandsen, S.L., Macechko, P.T., Van Keulen, H., and Jarroll, E.L. (1996) Formation of the *Giardia* cyst wall: studies on extracellular assembly using immunogold labeling and high resolution field emission SEM. *J. Euk. Microbiol.*, **43**, 416–429.

Ferguson, A., Gillon, J., and Munro, G. (1990) Pathology and pathogenesis of the intestinal mucosal damage in giardiasis. In: Meyer, E.A. (ed.), *Giardiasis*. Elsevier Science Publ. B.V., Amsterdam, pp. 155–174.

Gerwig, G.J., Kamerling, J.P., and Vliegenthart, J.F.G. (1979) Determination of the absolute configuration of monosaccharides in complex carbohydrates by capillary G.L.C. *Carbohydr. Res.*, **77**, 1–7.

Grootenhuis, P.D.J. and Haasnoot, C.A.G. (1993) A CHARMm based force field for carbohydrates using the CHEAT approach: carbohydrate hydroxyl groups represented by extended atoms. *Mol. Simul.*, **10**, 75–95.

Hooft, R.W.W., van Eijck, B.P., and Kroon, J. (1992) An adaptive umbrella sampling procedure in conformational analysis using molecular dynamics and its application to glycol. *J. Chem. Phys.*, **97**, 6690–6694.

IUPAC-IUB Joint Commission on Biochemical Nomenclature. (1983) Symbols for specifying the conformation of polysaccharide chains. *Eur. J. Biochem.*, **131**, 5–7.

Jarroll, E.L. and Paget, T.A. (1995) Carbohydrate and amino acid metabolism in *Giardia*: a review. *Folia Parasitol.*, **42**, 81–89.

Jarroll, E.L., Manning, P., Lindmark, D.G., Coggins, J.R., and Erlandsen, S.L. (1989) *Giardia* cyst wall-specific carbohydrate: evidence for the presence of galactosamine. *Mol. Biochem. Parasit.*, **32**, 121–132.

Kamerling, J.P. and Vliegenthart, J.F.G. (1989) Carbohydrates. In: Lawson, A.M. (ed.), *Clinical biochemistry—principles, methods, applications*, Vol. 1, *Mass spectrometry*. Walter de Gruyter, Berlin, pp. 176–263.

Kouwijzer, M.L.C.E. and Grootenhuis, P.D.J. (1995) Parametrization and application of CHEAT95, an extended atom force field for hydrated (oligo)saccharides. *J. Phys. Chem.*, **99**, 13426–13436.

Kouwijzer, M. and Perez, S. (1998) Molecular modeling of agarose helices, leading to the prediction of crystalline allomorphs. *Biopolymers*, **46**, 11–29.

Kroon-Batenburg, L.M.J., Kruiskamp, P.H., Vliegenthart, J.F.G., and Kroon, J. (1997) Estimation of the persistence length of polymers by MD simulations on small fragments in solution. Application to cellulose. *J. Phys. Chem. B*, **101**, 8454–8459.

Macechko, P.T., Steimle, P.A., Lindmark, D.G., Erlandsen, S.L., and Jarroll, E.L. (1992) Galactosamine synthesizing enzymes are induced when *Giardia* encyst. *Mol. Biochem. Parasitol.*, **56**, 301–310.

Manning, P., Erlandsen, S.L., and Jarroll, E.L. (1992) Carbohydrate and amino acid analyses of *Giardia muris* cysts. *J. Protozool.*, **39**, 290–296.

Paget, T.A., Macechko, P.T., and Jarroll, E.L. (1998) Metabolic changes in *Giardia intestinalis* during differentiation. *J. Parasitol.*, **84**, 222–226.

Rao, V.S.R., Qasba, P.K., Balaji, P.V., and Chandrasekaran, R. (1998) *Conformation of carbohydrates.* Amsterdam Harwood Academic Publishers.

Ryckaert, J.P., Ciccotti, G., and Berendsen, H.J.C. (1977) Numerical integration of the cartesian equations of motion of a system with constraints: molecular dynamics of n-alkanes. *J. Comput. Phys.*, **23**, 327–341.

Spieser, S.A.H., van Kuik, J.A., Kroon-Batenburg, L.M.J., and Kroon, J. (1999) Improved carbohydrate force field for GROMOS: ring and hydroxymethyl group conformations and exo-anomeric effect. *Carbohydr. Res.*, **322**, 264–273.

Van Gunsteren, W.F. (1987) GROMOS, Groningen molecular simulation package. University of Groningen, The Netherlands.

Van Keulen, H., Steimle, P.A., Bulik, D.A., Boroviak, R., and Jarroll, E.L. (1998) Cloning of two putative *Giardia lamblia* glucosamine 6-phosphate isomerase genes only one of which is transcriptionally activated during encystment. *J. Euk. Microbiol.*, **45**, 637–642.

Vliegenthart, J.F.G., Dorland, L., and van Halbeek, H. (1983) High-resolution, ^{1}H-nuclear magnetic resonance spectroscopy as a tool in the structural analysis of carbohydrates related to glycoproteins. *Adv. Carbohydr. Chem. Biochem.*, **41**, 209–374.

Ward, W., Alvarado, L., Rawlings, N.D., Engel, J.C., Franklin, C., and McKerrow, J. (1997) A primitive enzyme for a primitive cell: the protease required for excystation of *Giardia*. *Cell*, **89**, 437–444.

Wolfe, M. (1990) Clinical symptoms and diagnosis by traditional methods. In: Meyer, E.A. (ed.), *Giardiasis*. Elsevier Science Publ. B.V., Amsterdam, pp. 175–186.